Am J Transl Res 2021;13(7):7610-7621
www.ajtr.org /ISSN:1943-8141/AJTR0117818

Original Article

The role of T2E mediated CBF-1/RBP-Jκ signaling in metastatic thyroid cancer

An Hu[1], Fan-Fan Cao[2], Dan Lu[3], Li-Yun Yang[1]

[1]Department of Otolaryngology-Head and Neck Surgery, Gongli Hospital, Second Military Medical University, Pudong New Area, Shanghai 200135, China; [2]Sino-French Cooperative Central Lab, Gongli Hospital, Second Military Medical University, Pudong New District, Shanghai 200135, China; [3]Department of Otolaryngology-Head and Neck Surgery, Shanghai General Hospital, Shanghai Jiao Tong University School of Medicine, Shanghai, 200001, China

Received July 2, 2020; Accepted September 17, 2020; Epub July 15, 2021; Published July 30, 2021

Abstract: Objective: Cancer has been shown to be an independent risk factor for 2019-nCoV. Expression of transmembrane serine protease 2 (TMPRSS2) is abnormal in many cancers. Nevertheless, system analysis of TMPRSS2-ERG (T2E) abnormalities in metastatic thyroid cancer remains to be elucidated. Method: Using genomic and chromatin data, we demonstrate a unique cis-regulatory landscape between non-T2E and T2E-positive metastatic thyroid cancers, including clusters of regulatory elements (COREs). We attempt to describe the effect of T2E silencing on the cis-regulatory structure in metastatic thyroid cancers and its phase with the obvious phenotype characteristics of T2E-positive metastatic thyroid cancers. Results: These differences were linked by the ERG (erythroblast transformation-specific related gene) co-opts of FoxA1 and HOXB13, which realized T2E specific transcription profile. The study also demonstrated the T2E-specific CORE in an ERG site of structural rearrangement, which is due to the expansion of the T2E locus and contributes to its up-expression. Ultimately, we demonstrate that T2E-specific transcription profile is the basis of vulnerability of CBF-1/RBP-Jκ pathway. In fact, CBF-1/RBP-Jκ pathway inhibits the invasion and growth of T2E-positive thyroid tumors. Conclusion: This study indicates that the overexpression of ERG co-option has a unique cis-regulatory structure in T2E positive thyroid tumors, which induces drug dependence on CBF-1/RBP-Jκ signal. Our study solved the genetic and epigenetic variation of T2E in metastatic thyroid cancer for the first time. It is worth noting that further functional and clinical validation is needed as our study is a bioinformatics analysis.

Keywords: COVID-19, TMPRSS2, T2E, CBF-1/RBP-Jκ signaling, metastatic thyroid cancer

Introduction

Outbreak of a novel coronavirus disease (2019-nCoV) in 2019 has become the world's largest health threat [1-4]. At present, about 3,600,000 people have been infected worldwide, and more than 450 thousand lives have been lost [5]. In addition, cancer has been shown to be an independent risk factor for 2019-nCoV [6, 7]. The cell entry of coronavirus depends on the binding of spike protein to cell receptor and the activation of S protein of host cell protease [8]. Unravelling which cytokines are used by 2019-nCoV for entry might provide insight into reveal therapeutic targets and viral transmission [9]. Transmembrane serine Proteinase-2 (TMPRSS2) is a key factor leading to coronavirus infection including COVID-19 [10]. The mechanism of acute lung injury caused by COVID-19 infection might be related to TMPRSS2-ERG (T2E) [11]. T2E is not only widely expressed in lung [12, 13], but also in thyroid follicular epithelial cells [14]. Therefore, T2E related signaling pathway might also play a role in metastatic thyroid cancer.

Thyroid tumor is the most common noncortical cancer in women in the world [15]. Up-expression of transcription factor ERG is the most frequent somatic mutation in thyroid cancer, and the most common result of the fusion of T2E gene [16]. This fusion results in high expression of T2E, which is driven by the TSH response promoter of T2E gene. Compared with benign thy-

roid follicular epithelial cells, these lead to an increase in invasion and migration of follicular epithelial cells and incomplete differentiation [14].

In view of the influence of transcription factor ETS on remodeling chromatin and transcription factors [17, 18], its ability to accelerate the carcinogenic phenotype of thyroid tissues [19], and the known role of T2E as an initial transcription factor in many cell lines [20-23], we attempt to describe the effect of T2E silencing on the cis-regulatory structure in metastatic thyroid cancers and its phase with the obvious phenotype characteristics of T2E-positive metastatic thyroid cancers.

Materials and methods

ERG stratification and tumor samples

Sixteen fresh metastatic thyroid tumor tissues samples are obtained from thyroidectomy specimen from patient with thyroid tumor identified as moderate risk. These studies were approved by the medical ethics committee of the Affiliated Hospital and informed consent of all subjects or their relatives was obtained. The stratification of T2E-negative (non-T2E) or T2E-positive was determined by mRNA expression microarray data, and the positive detection was considered as T2E sample. The expression of ERG mRNA in a sample was divided into two groups by K-means clustering.

Cell culture

Three human papillary thyroid cancer cell lines (TPC-1, KTC-1 and NPA-87) were cultured in 10% FBS, in which 1% penicillin streptomycin and RPMI-1640 were cultured in incubator at 5% CO_2 and 37°C. All cells were detected for mycoplasma contamination and the results were negative. The cells were incubated for 48 hours before chromatin was harvested. SiRNAs (Thermo Fisher Scientific) were selected for knockdown test. Primers for genotyping TMPRSS2/ERG silence mouse strains (excised): GGA TCT GCT GGC ACG ATA ACT CTG.

Gene expression arrays

The matched samples were analyzed for mRNA by R statistical environment. Normalization algorithm, annotation and background correction are carried out in the oligo package (V3.0). Subsequently, the well-established limma (v3.22.6) package was used to calculate the differential gene expression to estimate the statistical significance (Bonferroni Holm correction, $Q \leq 0.05$). Invasive immune cells were estimated by R-packet Estimate of tumor stroma and immune cells by gene expression array.

H3K27ac ChIP in metastatic thyroid cancer

The fast-frozen specimens of metastatic thyroid cancer were cut into 20 μM sections (each ChIP uses 1-3 sections, depending on the tumor size) and fixed with PBS soaked at room temperature in 2% formaldehyde for ten minutes. After fixation, the tissue section was washed with ice-cold PBS or BSA/PBS. Then tissues were transferred to 200 μl of lysis buffer (pH8.1, 50 mM Tris-HCl, 1% SDS, 10 mM EDTA). Cell debris were removed by centrifugation at 3°C at 20000 r.p.m. for 10 min. 5 μL protein G and protein A Dynabeads per ChIP was washed 3 times in ice-cold BSA/PBS (0.01 g/l), then resuspend them in 250 μl ice-cold BSA/PBS, and add 2 μg antibody of H3-lysine-27ac.

RNA extraction and RT-qPCR

Total RNA was extracted from the samples using TRIzol reagent (Invitrogen, CA, USA) according to the manufacturer's instruction. According to the scheme recommended by the manufacturer, 1 μg RNA (The primer: GAG CAT TGC GGT TTA TCA AGC TGG) is reverse transcribed into cDNA using iScript cDNA synthesis kit. The quality and concentration of the RNA was tested in agarose gel electrophoresis and a NanoDrop ND-2000 spectrophotometer. The ΔΔCt value was calculated by subtracting the ΔCt of the reference sample from the ΔCt of each sample. The fold-change was determined as $2^{-\Delta\Delta Ct}$.

Migration assay and DAPT (2, 4-diamino-5-phenylthiazole) treatment

About one million NPA-87, TPC-1 or KTC-1 cells were plated in 24-well plates with 5 mL medium and 10 μM of DAPT (a chemical inhibitor of CBF-1/RBP-Jκ signal) or DMSO media, respectively. After 24 hours, NPA-87 cells were treated with trypsin, and 150,000 cells were inoculated into 24 transwells. The upper layer was 0.3

mL no-serum DMEM plus 6 μM DAPT or DMSO, and the lower layer was 500 μL FBS plus DMSO or 5 μM DAPT. Before fixation and crystal violet staining, the cell was allowed to migrate for 2 days. TPC-1 or KTC-1 cell was tryptized 2 days after transwell, and 4×10^4 cells were trans to 24-well plates, 0.3 ml no-serum RPMI plus DMSO or 5 μm DAPT were plated in the upper cavity, 0.5 ml RPMI was plated in the lower cavity, and 10% FBS + DMSO or 5 μm DAPT were plated in the lower cavity.

Xenograft and metastasis assays

About 2×10^6 living cells were inoculated subcutaneously into right flank of 5-7 weeks old nude mice. Metastatic thyroid tumor was removed from 24-30 weeks old TMPRSS2$^{-/-}$; TRAMP or TMPRSS2^{WT} mouse and transferred to no-phenol RPMI with antibiotic and 10% fetal bovine serum. The volume of the implanted tumor was measured at every 2 days with a vernier caliper, using the formula: $V = L \times W^2/2$; the mice experiments were terminated when tumors grew to a maximum of 400 mm^3. The tumors were removed and halved for immunohistochemical studies and Western blot analysis. The tissues were cut with a scalpel and passed through a 0.1 mM cells filter. Determination of the number of living cells by trypan blue exclusion.

Statistical analysis

All statistical analyses were performed using the statistical software package for Social Sciences (v. 13) (SPSS). Significance analyses of overlap between T2E-down and T2E-up regions and cell line transcription factor ChIP peaks was performed using Genome Structure Correction software. In comparison, the overlap of the significant boxes showed the same acetylation change direction was incorporated. We performed a two tailed Wilcoxon signed rank test between T2E and non-T2E samples of all linkage enhancers, and corrected by FDR. Wilcoxon rank sum test was used to analyze the difference of demographic characteristics between the two groups with different T2E expression. Pearson test was used to evaluate the correlation between CBF-1 expression and T2E expression. Two main clusters were identified by unsupervised hierarchical clustering based on CREs signals of each tumor, which were mainly separated based on over expression of ERG mRNA and T2E fusion. Student's t test was used to obtain the *p* value for comparison of line-linked groups. All statistical tests were bilateral, $P < 0.05$ was considered statistically significant.

Results

Correlation between active CREs (cis-regulatory elements) and T2E expression in metastatic thyroid tumors

We selected 16 metastatic thyroid tumors from a cohort of 286 patients that were previously evaluated for genomic changes. Unsupervised hierarchical clustering based on histone H3-lysine-27 acetylation signals identified two major clusters from each tumor of all CREs, mainly based on T2E fusion and mRNA up-expression of ERG (**Figure 1A**). The tumor with high ERG expression was aggregated from mRNA array data, and the evidence of gene rearrangement was considered as T2E positive (**Figure 1B**). About 11% of these CREs elements are located in the promoter, 47% in the intron region and 34% in the intergenic region (**Figure 1C**). This is consistent with the priority genome distribution of histone H3-lysine-27 acetylation on the active CREs enhancer and the promoter reported in other systems. Active elements in all 16 tumors, including thyroid function specific gene and housekeeper gene (**Figure 1D**). We identified 83,236 and 138,143 CREs enriched in H3-lysine-27 acetylation and 197,890 active CREs (**Figure 1E**). In a cohort of 286 patients with metastatic thyroid tumors, samples were clustered according to T2E status, which was compared with other common gene changes determined by whole genome sequencing. Other reported gene changes, including PTEN and TP53 deletions, were not directly and consistently associated with different chromatin landscapes in T2E tumors (**Figure 1F**). These studies suggest that the up-expression of ERG is preconditions for chromatin rearrangement of T2E metastatic thyroid cancers.

Specific chromatin and gene expression profile of T2E metastatic thyroid tumor

To describe how the change in chromatin rearrangement drive T2E metastatic thyroid tumor, we reported CREs that showed remarkable acetylation difference between non-T2E and T2E metastatic thyroid cancers. Most of the T2E-down or T2E-up elements are located at

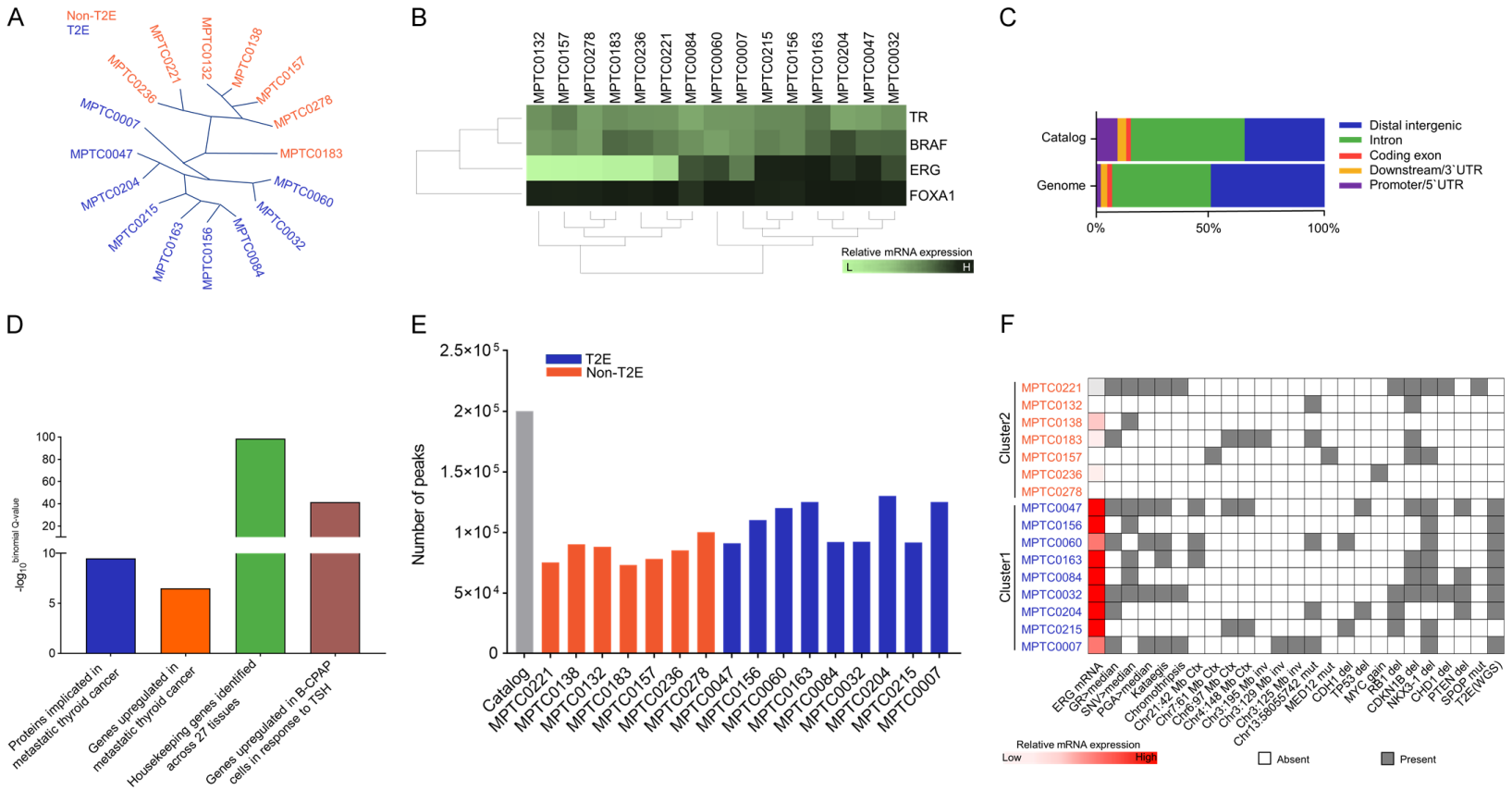

Figure 1. Histone H3-lysine-27 acetylation ChIP-seq defines the activity of CREs near the function related genes in metastatic thyroid tissue samples. A. Unsupervised hierarchical clustering of 7 cases of non-T2E and 9 cases of T2E cancers using the cluster of ChIP-seq of H3K27ac. B. Full linkage hierarchical cluster analysis of BRAF, TR, FoxA1 and ERG gene express levels in 15 metastatic thyroid cancer patients. C. Distribution of H3K27 acetylated enriched CREs in promoter, exon, intron, downstream or promoter 5'UTR and 3'UTR element of the gene and CRE of 16 tumors. D. GREAT (Genomic Regions Enrichment of Annotations Tool) analysis of H3-lysine-27 acetylation peak was consistent in 16 tumors. Q value (housekeeping gene) and significant thyroid specific description from MSigDB disturbance ontology are shown (observed/expected fold changes > 2). E. The total number of CREs enriched by acetylation of H3K27 in 16 metastatic thyroid tissue samples (9 T2E, 7 non-T2E). F. Common mutations or copy number abnormalities of thyroid cancer were found in the whole genome sequencing data of 16 samples analyzed by ChIP-seq cluster analysis of H3K27ac. It also includes log2 value of ERG mRNA expression microarray data.

the far end of the promoter, which is a typical enhancer, while the same active element in the subtype is twice the promoter (**Figure 2A**). Unsupervised hierarchical clustering based on the express level of gene could also distinguish non-T2E from T2E metastatic thyroid tumors (**Figure 2B**). Compared with non-T2E samples, we found that 807 CREs binding components in T2E tumor showed higher acetylation level, while 1,023 CREs binding components in T2E tumor showed lower acetylation level (negative binomial test, FDR-corrected, $q \leq 0.05$) (**Figure 2C**). The expression data of matched tumor genes analyzed by H3-lysine-27 acetylation microarray showed that the expression of genes related to T2E-up promoter or enhancer was significantly increased in T2E tumor, while that of genes related to T2E-down promoter or enhancer was decreased in T2E tumor (**Figure 2D**, **2E**) (FDR-corrected, $Q \leq 0.05$).

T2E activates c-Met signal to participate in the chromatin rearrangement that contribute to metastasis

Because bFGF signal transduction promotes epithelial to mesenchymal transfer (EMT), we detected gene expression of this phenotype. We first confirmed the expression of TMPRSS2 and c-Met in primary and metastatic TMPRSS2^{wt} tumors (**Figure 3A**). Tumors with positive immunohistochemical staining or gene rearrangement are considered (**Figure 3B**). Next, we dissected the normal thyroid epithelium of wild-type animals and the epithelium of TMPRSS2$^{-/-}$ and TMPRSS2^{wt} thyroid tumors. According to the clustering analysis, the expression level of EMT (epithelial-mesenchymal transition) related genes in TMPRSS2$^{+/+}$ was significantly higher (**Figure 3C**). The study shown that bFGF signal could inhibit cell invasive and enhance proliferation phenotype at the same time. In order to compare the abundances of these proteases directly, we dissected the tumor epithelium of metastatic thyroid cancer ($n = 36$) and localized thyroid cancer ($n = 18$), and quantitatively analyzed the transcription level of the cancer. We found that the level of T2E exceeded that of Hepsin and Matriptase in most thyroid cancers ($p < 0.01$) (**Figure 3D**). High level of T2E in invasive thyroid cancer promotes further study of the role of T2E in metastasis (**Figure 3E**). The expression of proliferating nuclear antigen (PCNA), p27 and p21 were up-regulated by bFGF in TCP-1 cells, while the express level of PCNA in KTC-1 cells increased (**Figure 3F**, **3G**).

ERG overexpression regulates TR, HOXB13 and FoxA1 cistromes

Cell characteristics are obviously correlated with the interaction between chromatin landscape and transcription factor activity. Therefore, this study demonstrated the effect of ERG up-expression on chromatin landscape in T2E metastatic thyroid cancers, because it is related to the structure of other transcription factor. Notably, metastatic thyroid tumors presented with increased ACE2 expression (**Figure 4A**). Analysis of differential expression in patients with high and low levels of ERG showed that HDAC1 was one of the top 10 up-regulated transcripts in high-level ERG samples, as shown in **Figure 4B**. Next, we compared the expression of ACE2 in tumor and normal control tissues. Compared with the whole genome background, the shared CREs of forkhead (FKH), TSH response element (TRE) and homeobox (HBOX) motifs are more abundant (**Figure 4C**). Western blot study indicated that there was little change in FoxA1 and HOXB13 protein expression after ERG gene knockout (**Figure 4D**). Therefore, the out of context overexpression of ERG seems to shift the core mechanism of thyroid tumors transcription to a new set of CREs, similar to its physical connection and regulation with modulate partner transcription factors in endothelial cell and hematopoietic environments.

ERG specific CREs activated by CBF-1/RBP-Jκ pathway

The lack of treatment for ERG leads us to search for an operable target for activation of ERG up-expression in T2E metastatic thyroid cancers. This study evaluated the changes of H3-lysine-27 acetylation level at the T2E-down and T2E-up genes after the removal of ERG in NPA-87 cells by siRNA to determine the ERG dependent CREs. We observed that the acetylation level of H3-lysine-27 decreased significantly when T2E-up CREs by 18.0%, and increased significantly when T2E-down CREs by 8.7% (**Figure 5A**). Analysis of acetylated elements of ERG dependent H3-lysine-27 by GREAT (Genomic Regions Enrichment of Annotations Tool) analysis shows enrichment of

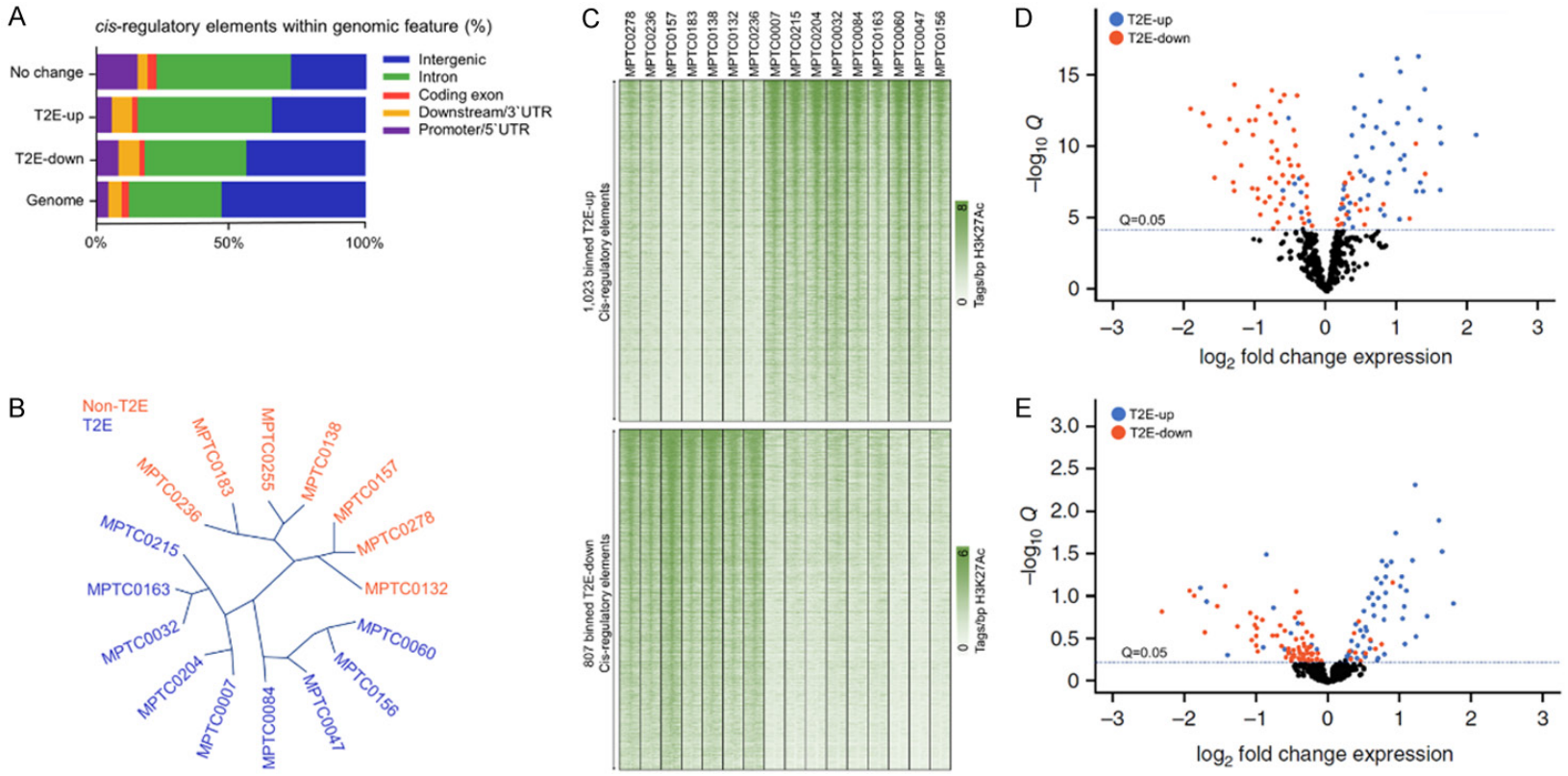

Figure 2. T2E metastatic thyroid tumor has obvious gene expression profile and chromatin. A. Genome distribution of promoter, exon, intron, promoter/5'UTR and downstream/3'UTR elements, T2E-down CREs, T2E-up CRE or CREs without H3-lysine-27 acetylation. B. Unsupervised hierarchical clustering was performed in 7 non-T2E and 9 T2E cancers using the standardized express levels of genome express chip. C. H3k27ac signal thermogram of T2E-down and T2E-up element in 16 patients. D. The -log10 FDR vs. log2 fold change corrected the statistical significance Q value of tumors analyzed by h3k27ac ChIP-seq, in which promoter was covered by T2E-down and T2E-up regulate elements. E. Q value vs. Log2 fold change to statistically analyze all genes related to metastatic T2E-down and T2E-up regulate element of tumor from h3k27ac ChIP-seq.

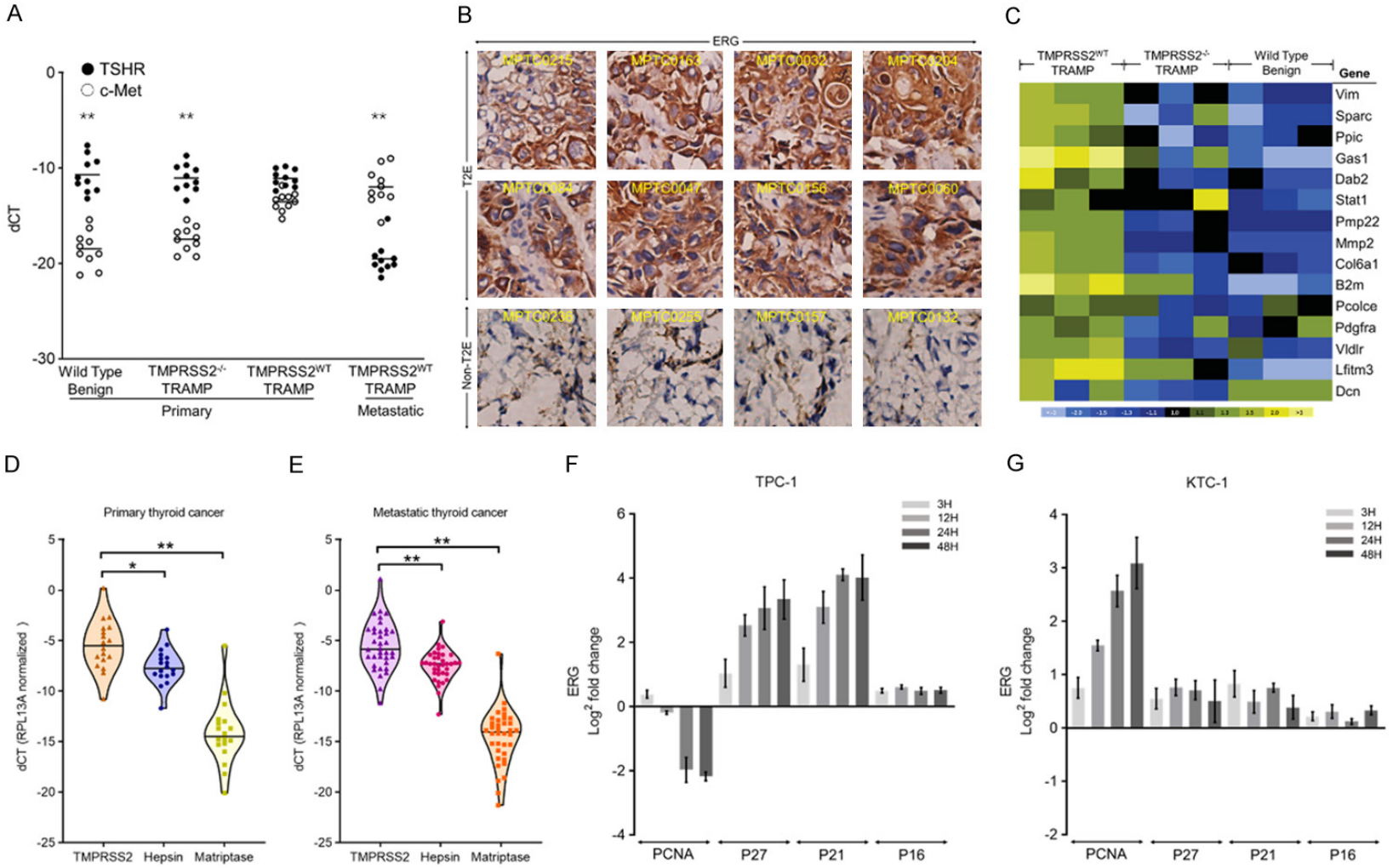

Figure 3. T2E-activated bFGF continued to promote invasion but increased or inhibited proliferation in varying degrees. A. Detection of c-Met and TSHR transcription in metastatic or primary TRAMP cancers by qRT-PCR. B. Immunohistochemistry of ERGs in 4 non-T2E and 8 T2E metastatic thyroid cancer specimens. C. Microarray-based transcript profiling analysis of mRNAs in thyroid epithelium. EMT related genes increased in TMPRSS2$^{+/+}$ RAMP tumors, and decreased in TMPRSS2$^{-/-}$ TRAMP tumors. D, E. Detection of T2E, Hepsin and Matriptase mRNA expression in primary thyroid cancer and metastasis of advanced thyroid cancer by qRT-PCR. F, G. The effect of bFGF activation on cell cycle regulators p27 and P21 of TPC-1 and KTC-1 cells.

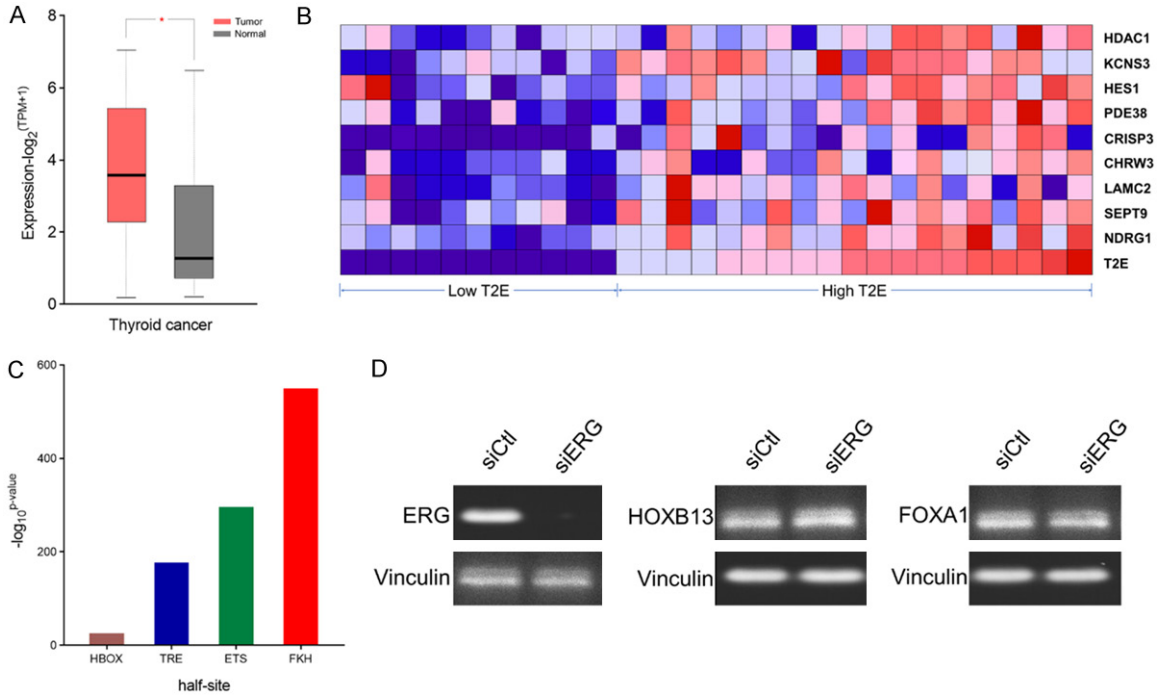

Figure 4. In patients with metastatic thyroid cancer the expression levels of ERG and HDAC are correlated. A. Increased expression of ACE2 in metastatic thyroid tumors. *P < 0.05. grey, normal control sample; Red, tumor sample. B. The top 10 up regulated transcriptional datasets were divided into low (n = 11, average 97.1, maximum 130) and high (n = 19, average 698, minimum 380) ERG expression samples. C. There was no remarkable distinguish in enrichment of cis-regulatory elements between non-T2E and T2E tumor (HBOX: homebox; ETS: E26 transformation specific; TRE: TSH response element; FKH: Forkhead). D. Western blots study of HOXB13, FoxA1 and ERG in NAP-87 cells after siRNA deletion of ERG. Immunoblotting was used as the loading control. (siERG: ERG targeted siRNA; siCtl: non-targeted siRNA).

CBF-1/RBP-Jκ signaling pathway (**Figure 5B**). In addition, up regulation of JAG1, HES1 and DLL1 mRNA is a typical feature of T2E positive thyroid tumors in the thyroid cancer cohort (**Figure 5C-E**). Considering the over expression of ERG promotes the migration and invasion of thyroid cancer cells, a chemical inhibitor of CBF-1/RBP-Jκ signal (DAPT) was used to treat KTC-1, NAP-87 and TPC-1 cells. We observed a 25% decrease in the migration of T2E-negative KTC-1 and NAP-87 cells and a 35% decrease in the migration of TPC-1 cells (**Figure 5F**, **5G**). In conclusion, our results support that in T2E metastatic thyroid tumors, the expression of CBF-1/RBP-Jκ is increased due to the ERG dependent activation of T2E.

Discussion

Spike protein of 2019-nCoV promotes virus entry into target cell [24, 25]. SARS-S uses ACE2 as the target receptor, and spike protein is activated by TMPRSS2 [26]. Nearly 72% of thyroid cancer patients have T2E subtypes [14], and the overexpression of ERG has been thought to drive tumor development. Frequent deletions extend the core containing the T2E promoter to the rearranged ERG allele [27, 28]. The CORE of this expansion includes CREs, which is involved in some of the ERG loci and promotes the over expression of ERG [29]. Previous studies have shown that point mutations can cause oncogene driven COREs, whereas rearrangement and amplification of COREs could enhance oncogene expression [21, 30]. As far as we know, these studies indicate for the first time that the expansion of COREs after chromosome rearrangement has a significant impact on the express level of target genes.

Because of the over expression of ERG, there is a dependent cis-regulatory cluster in T2E metastatic thyroid cancers [31, 32], suggesting that ERG can alter chromatin rearrangement. These data are consistent with and based on the pub-

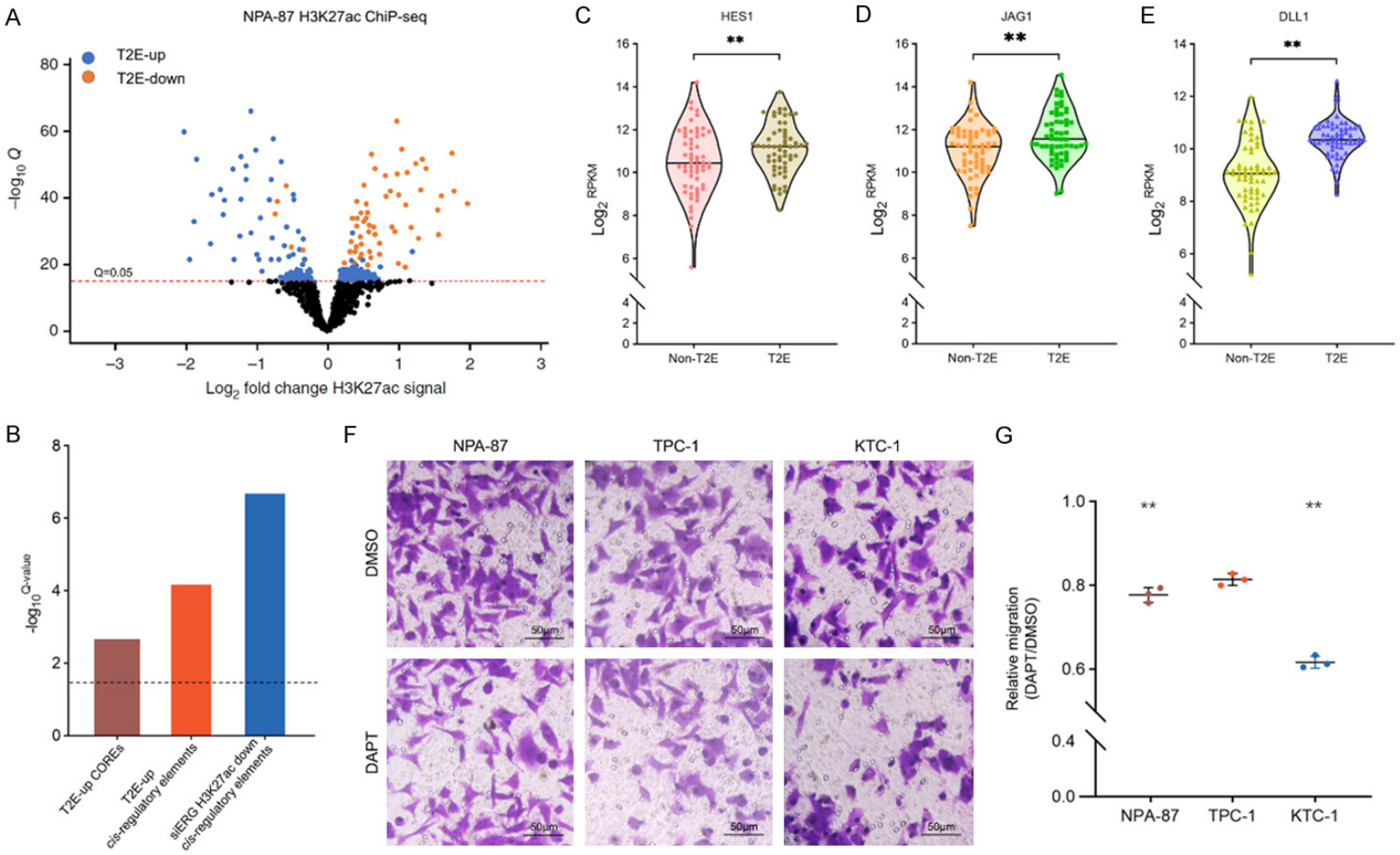

Figure 5. ERG activates CREs around CBF-1/RBP-Jκ pathway gene. A. Volcanic map of the Q-value corrected by -log10 FDR and the log2 fold change of acetylated of H3-lysine-27 during ERG knockout in NPA-87 cells (three independent copies in each group). B. -Log_{10} FDR-corrected Q-value, which is used to calculate and enrich the regulation of CBF-1/RBP-Jκ signal pathway by CRE with tissues identified CORE or T2E-up CRE and significantly loss of activities after ERGs gene knockout. C-E. Expression of DLL1, JAG1 and HES1 mRNA in non-T2E or T2E sample from TCGA thyroid tumor cluster. F. After DMSO or DAPT treatment, the transmembrane cells stained with crystal violet migrated to NPA-87, TPC-1 and KTC-1 cells. G. Quantitative results of transwell migration with three independent repeats. *$P < 0.05$, two-tailed, one-sample t-test, Bonferroni-corrected; **$P < 0.01$, two-tailed t-test, Bonferroni-corrected.

lished results [32]. These data show that ERG can induce the overall changes of chromatin topology, thus promoting the expression of ERG target gene in thyroid epithelial cells, which indicates that ERG can not only promote the cis-regulation of chromatin interaction, but also promote the activity of chromatin landscape [33, 34]. In addition, our data are consistent with the ability of ETS factors ELK3 and ETS2 to regulate the level of H3K27ac in CREs.

Finally, this study shows the activation of CBF-1/RBP-Jκ pathway in T2E metastatic thyroid tumors. CBF-1/RBP-Jκ signal transduction promotes the maintenance and proliferation of stem cell in the development of thyroid cancer [35], while the inhibition of CBF-1/RBP-Jκ signal transduction reduces the growth and invasion of cells in thyroid cancer. Our results show that CBF-1/RBP-Jκ signal is involved in the invasive characteristics of T2E thyroid tumor stem cell. Therefore, the reducing of CBF-1/RBP-Jκ pathway could provide treatment method against the metastasis phenotype of T2E thyroid tumor. In addition, in COVID-19 patients with T2E, tumor tissue may be more susceptible to SARS-CoV-2 infection, thus worsening the prognosis [36, 37]. Since these studies are only preliminary analysis, it is worth further verification in larger clinical samples.

Acknowledgements

This study was supported by the Shanghai Pudong Science & Technology Project (No. PW2017A-20); Key Disciplines Group Construction Project of Pudong Health Bureau of Shanghai (No. PWZxq2017-04); Research Grant for Health Science and Technology of Pudong Health Bureau of Shanghai (No. PW-2019D-4) and Key Specialty Construction Project of Health Bureau of Shanghai (No. ZK2019C06).

Disclosure of conflict of interest

None.

Address correspondence to: An Hu, Gongli Hospital, Second Military Medical University, Pudong New Area, Miaopu Road 219, Shanghai 200135, China. Tel: +86-13764147286; E-mail: juanitohuan@sjtu.edu.cn

References

[1] Wrapp D, Wang N, Corbett KS, Goldsmith JA, Hsieh CL, Abiona O, Graham BS and McLellan JS. Cryo-EM structure of the 2019-nCoV spike in the prefusion conformation. Science 2020; 367: 1260-1263.

[2] Li G and De Clercq E. Therapeutic options for the 2019 novel coronavirus (2019-nCoV). Nat Rev Drug Discov 2020; 19: 149-150.

[3] Carlos WG, Dela Cruz CS, Cao B, Pasnick S and Jamil S. Novel Wuhan (2019-nCoV) coronavirus. Am J Respir Crit Care Med 2020; 201: P7-P8.

[4] Yuan W, Liu S, Lu L, Feng J and He X. Clinical interventions for severe and critical COVID-19: what are the options. Am J Transl Res 2020; 12: 2110-2117.

[5] WHO. Novel coronavirus (2019-nCoV) situation report 23. 2020.

[6] Liang W, Guan W, Chen R, Wang W, Li J, Xu K, Li C, Ai Q, Lu W, Liang H, Li S and He J. Cancer patients in SARS-CoV-2 infection: a nationwide analysis in China. Lancet Oncol 2020; 21: 335-337.

[7] Huang B, Zhu J, Wu XY and Gao XH. Should patients stop their radiotherapy or chemotherapy during the COVID-19 pandemic. Am J Cancer Res 2020; 10: 1518-1521.

[8] Tian S, Hu W, Niu L, Liu H, Xu H and Xiao SY. Pulmonary pathology of early-phase 2019 novel coronavirus (COVID-19) pneumonia in two patients with lung cancer. J Thorac Oncol 2020; 15: 700-704.

[9] Xia Y, Jin R, Zhao J, Li W and Shen H. Risk of COVID-19 for patients with cancer. Lancet Oncol 2020; 21: e180.

[10] Stopsack KH, Mucci LA, Antonarakis ES, Nelson PS and Kantoff PW. TMPRSS2 and COVID-19: serendipity or opportunity for intervention? Cancer Discov 2020; 10: 779-782.

[11] Peters MC, Sajuthi S, Deford P, Christenson S, Rios CL, Montgomery MT, Woodruff PG, Mauger DT, Erzurum SC, Johansson MW, Denlinger LC, Jarjour NN, Castro M, Hastie AT, Moore W, Ortega VE, Bleecker ER, Wenzel SE, Israel E, Levy BD, Seibold MA and Fahy JV. COVID-19-related genes in sputum cells in asthma. relationship to demographic features and corticosteroids. Am J Respir Crit Care Med 2020; 202: 83-90.

[12] Rotllan N, Wanschel AC, Fernández-Hernando A, Salerno AG, Offermanns S, Sessa WC and Fernández-Hernando C. Genetic evidence supports a major role for Akt1 in VSMCs during atherogenesis. Circ Res 2015; 116: 1744-1752.

[13] Reid JC, Matsika A, Davies CM, He Y, Broomfield A, Bennett NC, Magdolen V, Srinivasan B,

Clements JA and Hooper JD. Pericellular regulation of prostate cancer expressed kallikrein-related peptidases and matrix metalloproteinases by cell surface serine proteases. Am J Cancer Res 2017; 7: 2257-2274.
[14] Mirhosseini N, Brunel L, Muscogiuri G and Kimball S. Physiological serum 25-hydroxyvitamin D concentrations are associated with improved thyroid function-observations from a community-based program. Endocrine 2017; 58: 563-573.
[15] Naoum GE, Morkos M, Kim B and Arafat W. Novel targeted therapies and immunotherapy for advanced thyroid cancers. Mol Cancer 2018; 17: 51.
[16] Kim MJ, Sun HJ, Song YS, Yoo SK, Kim YA, Seo JS, Park YJ and Cho SW. CXCL16 positively correlated with M2-macrophage infiltration, enhanced angiogenesis, and poor prognosis in thyroid cancer. Sci Rep 2019; 9: 13288.
[17] Bullock M, Lim G, Zhu Y, Åberg H, Kurdyukov S and Clifton-Bligh R. ETS Factor ETV5 activates the mutant telomerase reverse transcriptase promoter in thyroid cancer. Thyroid 2019; 29: 1623-1633.
[18] Birdsey GM, Shah AV, Dufton N, Reynolds LE, Osuna Almagro L, Yang Y, Aspalter IM, Khan ST, Mason JC, Dejana E, Göttgens B, Hodivala-Dilke K, Gerhardt H, Adams RH and Randi AM. The endothelial transcription factor ERG promotes vascular stability and growth through Wnt/β-catenin signaling. Dev Cell 2015; 32: 82-96.
[19] Peyret V, Nazar M, Martín M, Quintar AA, Fernandez EA, Geysels RC, Fuziwara CS, Montesinos MM, Maldonado CA, Santisteban P, Kimura ET, Pellizas CG, Nicola JP and Masini-Repiso AM. Functional toll-like receptor 4 overexpression in papillary thyroid cancer by MAPK/ERK-induced ETS1 transcriptional activity. Mol Cancer Res 2018; 16: 833-845.
[20] Kron KJ, Murison A, Zhou S, Huang V, Yamaguchi TN, Shiah YJ, Fraser M, van der Kwast T, Boutros PC, Bristow RG and Lupien M. TMPRSS2-ERG fusion co-opts master transcription factors and activates NOTCH signaling in primary prostate cancer. Nat Genet 2017; 49: 1336-1345.
[21] Eryilmaz IE, Aytac Vuruskan B, Kaygısız O, Egeli U, Tunca B, Kordan Y and Cecener G. RNA-based markers in biopsy cores with atypical small acinar proliferation: predictive effect of T2E fusion positivity and MMP-2 upregulation for a subsequent prostate cancer diagnosis. Prostate 2019; 79: 195-205.
[22] Eryilmaz IE, Kordan Y, Vuruskan BA, Kaygısız O, Tunca B and Cecener G. T2E (TMPRSS2-ERG) fusion transcripts are associated with higher levels of AMACR mRNA and a subsequent prostate cancer diagnosis in patients with atypical small acinar proliferation. Gene 2018; 645: 69-75.
[23] Egbers L, Luedeke M, Rinckleb A, Kolb S, Wright JL, Maier C, Neuhouser ML and Stanford JL. Obesity and prostate cancer risk according to tumor TMPRSS2: ERG gene fusion status. Am J Epidemiol 2015; 181: 706-713.
[24] Xu J, Cheng Y, Yuan X, Li WV and Zhang L. Trends and prediction in daily incidence of novel coronavirus infection in China, Hubei Province and Wuhan City: an application of Farr's law. Am J Transl Res 2020; 12: 1355-1361.
[25] Gralinski LE and Menachery VD. Return of the coronavirus: 2019-nCoV. Viruses 2020; 12: 135.
[26] Richardson P, Griffin I, Tucker C, Smith D, Oechsle O, Phelan A, Rawling M, Savory E and Stebbing J. Baricitinib as potential treatment for 2019-nCoV acute respiratory disease. Lancet 2020; 395: e30-e31.
[27] Geybels MS, McCloskey KD, Mills IG and Stanford JL. Calcium channel blocker use and risk of prostate cancer by TMPRSS2: ERG gene fusion status. Prostate 2017; 77: 282-290.
[28] Geybels MS, Alumkal JJ, Luedeke M, Rinckleb A, Zhao S, Shui IM, Bibikova M, Klotzle B, van den Brandt PA, Ostrander EA, Fan JB, Feng Z, Maier C and Stanford JL. Epigenomic profiling of prostate cancer identifies differentially methylated genes in TMPRSS2: ERG fusion-positive versus fusion-negative tumors. Clin Epigenetics 2015; 7: 128.
[29] Ohta Y, Okabe T, Larmour C, Di Rocco A, Maijenburg MW, Phillips A, Speck NA, Wakitani S, Nakamura T, Yamada Y, Enomoto-Iwamoto M, Pacifici M and Iwamoto M. Articular cartilage endurance and resistance to osteoarthritic changes require transcription factor Erg. Arthritis Rheumatol 2015; 67: 2679-2690.
[30] Nakanuma Y, Uesaka K, Miyayama S, Yamaguchi H and Ohtsuka M. Intraductal neoplasms of the bile duct. A new challenge to biliary tract tumor pathology. Histol Histopathol 2017; 32: 1001-1015.
[31] Gerke JS, Orth MF, Tolkach Y, Romero-Pérez L, Wehweck FS, Stein S, Musa J, Knott MML, Hölting TLB, Li J, Sannino G, Marchetto A, Ohmura S, Cidre-Aranaz F, Müller-Nurasyid M, Strauch K, Stief C, Kristiansen G, Kirchner T, Buchner A and Grünewald TGP. Integrative clinical transcriptome analysis reveals TMPRSS2-ERG dependency of prognostic biomarkers in prostate adenocarcinoma. Int J Cancer 2020; 146: 2036-2046.
[32] García-Flores M, Casanova-Salas I, Rubio-Briones J, Calatrava A, Domínguez-Escrig J, Rubio L, Ramírez-Backhaus M, Fernández-Serra A,

García-Casado Z and López-Guerrero JA. Clinico-pathological significance of the molecular alterations of the SPOP gene in prostate cancer. Eur J Cancer 2014; 50: 2994-3002.

[33] Elemento O, Rubin MA and Rickman DS. Oncogenic transcription factors as master regulators of chromatin topology: a new role for ERG in prostate cancer. Cell Cycle 2012; 11: 3380-3383.

[34] Rickman DS, Soong TD, Moss B, Mosquera JM, Dlabal J, Terry S, MacDonald TY, Tripodi J, Bunting K, Najfeld V, Demichelis F, Melnick AM, Elemento O and Rubin MA. Oncogene-mediated alterations in chromatin conformation. Proc Natl Acad Sci U S A 2012; 109: 9083-9088.

[35] Yong T, Sun A, Henry MD, Meyers S and Davis JN. Down regulation of CSL activity inhibits cell proliferation in prostate and breast cancer cells. J Cell Biochem 2011; 112: 2340-2351.

[36] Khoury M, Cuenca J, Cruz FF, Figueroa FE, Rocco PRM and Weiss DJ. Current status of cell-based therapies for respiratory virus infections: applicability to COVID-19. Eur Respir J 2020; 55: 2000858.

[37] Kimura H, Francisco D, Conway M, Martinez FD, Vercelli D, Polverino F, Billheimer D and Kraft M. Type 2 inflammation modulates ACE2 and TMPRSS2 in airway epithelial cells. J Allergy Clin Immunol 2020; 146: 80-88.